Stability and Folding Kinetics of a Ubiquitin Mutant with a Strong Propensity for Nonnative β-Hairpin Conformation in the Unfolded State†

Geoffrey W. Platt,‡ Stephen A. Simpson,‡ Robert Layfield,§ and Mark S. Searle*,‡

School of Chemistry, University Park, Nottingham, NG7 2RD, United Kingdom, and School of Biomedical Sciences, Queen's Medical Centre, University of Nottingham, Nottingham, NG7 2UH United Kingdom

Received June 12, 2003; Revised Manuscript Received September 2, 2003

ABSTRACT: A F45W mutant of yeast ubiquitin has been used as a model system to examine the effects of nonnative local interactions on protein folding and stability. Mutating the native TLTGK G-bulged type I turn in the N-terminal β-hairpin to NPDG stabilizes a nonnative β-strand alignment in the isolated peptide fragment. However, NMR structural analysis of the native and mutant proteins shows that the NPDG mutant is forced to adopt the native β-strand alignment and an unfavorable type I NPDG turn. The mutant is significantly less stable (∼9 kJ mol^{-1}) and folds 30 times slower than the native sequence, demonstrating that local interactions can modulate protein stability and that attainment of a nativelike β-hairpin conformation in the transition state ensemble is frustrated by the turn mutations. Surprising, alcoholic cosolvents [5−10% (v/v) TFE] are shown to accelerate the folding rate of the NPDG mutant. We conclude, backed-up by NMR data on the peptide fragments, that even though nonnative states in the denatured ensemble are highly populated and their stability further enhanced in the presence of cosolvents, the simultaneous increase in the proportion of nativelike secondary structure (hairpin or helix), in rapid equilibrium with nonnative states, is sufficient to accelerate the folding process. It is evident that modulating local interactions and increasing nonnative secondary structure propensities can change protein stability and folding kinetics. However, nonlocal contacts formed in the global cooperative folding event appear to determine structural specificity.

How the information contained within the primary amino acid sequence is used to specify the topology of the native state of a protein, its stability, and the pathway by which the chain assembles to the native conformation continues to be the subject of much experimental and theoretical investigation (*1*−*4*). Globular proteins have the distinguishing features of large amounts of regular secondary structure and a hydrophobic core formed from tertiary contacts between these substructures when packed together. However, whether local contacts within the polypeptide chain specify secondary structure propensities in the folded state or whether secondary structure formation is dictated by nonlocal tertiary interactions as a consequence of the global cooperative folding event remains an important issue. Several studies have examined the influence of nonlocal factors in determining conformation. In one case, the same 11 residue sequence, unstructured in isolation, was shown to adopt either a β-sheet or an α-helix when placed in different contexts within the G_{B1} domain, illustrating the influence of tertiary contacts in driving secondary structure formation (*5*). Alternatively, substituting one native element of secondary structure with a sequence having a propensity for adopting an alternative conformation in isolation has also shown that preserved tertiary contacts appear to drive native secondary structure formation (*6*).

Whether these mutations affect folding kinetics depends to what extent the substituted element of secondary structure is involved in interactions in the transition state (*7*, *8*). Reinforcement of the folding nucleus by promoting native contacts should have the effect of accelerating folding. This has been demonstrated in a number of ways by introducing an autonomously folding component such as a β-hairpin (*9*) or through mutations that increase secondary structure propensities without perturbing tertiary interactions (*10*−*13*). Others have shown that the folding pathway can be altered by changing the relative stability of different elements of secondary structure (*14*). The observations to date are consistent with a hierarchical model for folding in which local events, resulting in progressive formation of nativelike contacts, play a central role. Alternatively, stabilizing the nonnative conformation in a portion of the sequence that is involved in interactions in the transition state may retard or frustrate folding by making attainment of the transition state structure energetically more costly (*6*, *15*).

We have examined this latter possibility in the context of the stability and folding of yeast ubiquitin (*16*). Ubiquitin has proved to be a paradigm for stability and folding studies on account of its small size (76 residues), high solubility, robustness to mutations, and reversibility of its folding/

† G.W.P. thanks the EPSRC and GlaxoSmithKline for financial support. S.A.S. is supported by the EPSRC through a Biomolecular Sciences Committee studentship. We are grateful to the EPSRC and the School of Chemistry for funding instrumentation. R.L. is supported by the Wellcome Trust.

* Corresponding author. E-mail: mark.searle@nottingham.ac.uk. Tel: 0115 951 3567.

‡ School of Chemistry.

§ University of Nottingham.

10.1021/bi030147d CCC: $25.00
Published on Web 10/25/2003

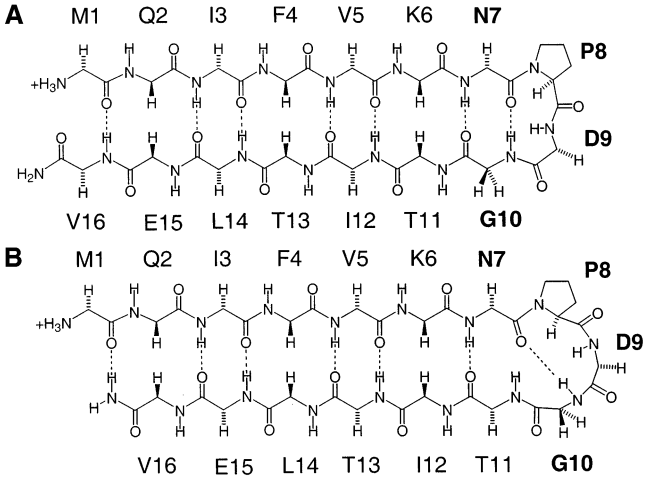

FIGURE 1: Peptide backbone alignment in the N-terminal β-hairpin containing the TLTGK → NPDG β-turn mutations: (A) native β-strand alignment found in the folded protein (yU$^{\beta}$) with an enforced type I turn and (B) preferred nonnative conformation in the isolated N-terminal fragment U(1−35) with a G-bulged type I turn and nonnative cross-strand pairing of residues. Residue numbering beyond G10 is $i - 1$ with respect to the native sequence. Residue side chains have been omitted for clarity.

unfolding transition (*17*−*21*). Recent investigations have examined the role of helix capping motifs (*22*), hydrophobic packing (*23*, *24*), and the influence of surface electrostatic interactions on stability (*25*, *26*). The N-terminal β-hairpin has been proposed to be a key structural element in the folding transition state of ubiquitin on the basis of NMR studies of the isolated 17 residue fragment that demonstrates a weak ability to fold autonomously in solution (*27*, *28*). In an attempt to further stabilize this element of secondary structure to reinforce the transition state for folding, we have mutated the TLTGK type I G-bulged turn sequence. Replacement of the native turn sequence with a type I NPDG turn results in a significantly stabilized β-hairpin peptide; however, detailed NMR analysis shows that it folds into a nonnative conformation in water in which there is a one residue frameshift in the β-strand alignment resulting in nonnative cross-strand residue pairing (Figure 1) (*29*, *30*). We have inserted the TLTGK → NPDG turn mutation into the native yeast ubiquitin structure to investigate its impact on the structure, stability, and folding pathway. We examine the role of nonlocal interactions in dictating secondary structure propensity, in particular β-strand alignment, through NMR structural analysis of the mutant and have determined the effects of the turn mutation on protein stability and kinetics. We examine the extent to which nonnative conformation in the unfolded state frustrates folding by carrying out a full kinetic analysis of the wild-type and mutant protein and one other β-turn mutant (TLTGK → NPDGK) designed to dissect out the contribution to stability of tertiary contacts involving β-turn residues.

MATERIALS AND METHODS

Peptides and Proteins. Peptide U(1−35) was prepared using standard Fmoc solid-phase methods and was purified using reverse-phase HPLC. A pKK223-3 plasmid construct containing the yeast ubiquitin gene was used to express the wild-type protein in *Escherichia coli* strain BL21(DE3) under the control of the IPTG-inducible *tac* promoter. Cells were grown at 37 °C in Luria broth (LB)/ampicillin (100 μg mL^{-1}) to mid-log stage and harvested 4 h after induction. Cells were resuspended in 50 mM acetate buffer, pH 4 containing 2 mM EDTA (AE). Cells were lysed by sonication and centrifuged. Addition of 250 mM acetate buffer to the supernatant precipitated a large proportion of the cellular proteins leaving ubiquitin in solution. Following centrifugation, the supernatant containing the remaining soluble cellular proteins was filtered and then chromatographed on a HiTrap SP cation exchange column with a 5 mL bed volume on an AKTA Prime FPLC system (Amersham Pharmacia Biotech). The sample was loaded on the column, washed with 50 mL of AE, and then eluted with an 80 mL linear gradient from 0 to 800 mM NaCl. Ubiquitin eluted at approximately 550 mM NaCl. Fractions containing ubiquitin were pooled and loaded onto a gel filtration column (Superdex 75) equilibriated with 30 mM phosphate buffer and 100 mM NaCl at pH 7.0. Fractions were assayed for ubiquitin by polyacrylamide gel electrophoresis. Fractions containing pure ubiquitin were pooled, dialyzed against distilled water, and lyophilized. The F45W mutant gene was cloned by overlap PCR methodology using the wild-type yeast ubiquitin gene in pKK223-3 (Pharmacia Biotech) as a template. The mutated cassette was inserted between the *Eco*RI and *Hin*dIII restriction sites of pKK223-3, and the mutation was confirmed by DNA sequencing. Competent *E. coli* cells were transformed with this construct. Expression and purification were as described for the wild-type yielding typically 10−15 mg L^{-1} of ubiquitin. Mutants were prepared by the same method. ^{15}N-Labeled yU$^{\beta}$ was prepared by growing BL21 cells in minimal medium containing $^{15}NH_4Cl$ (0.7 g L^{-1}) as the sole source of nitrogen. The protein was purified using the standard procedure.

NMR Analysis of Peptide and Protein Folding. All NMR experiments were performed on a Bruker Avance600 spectrometer. Total correlation spectroscopy (TOCSY) and nuclear Overhauser effect spectroscopy (NOESY) experiments collected 1024−2048 data points in *f*2 and 400−600 in *f*1 on 1 mM samples of the peptides at pH 2.2−5.5 and ubiquitin mutants at pH 5.5. Solvent suppression was achieved by presaturation of the water signal for samples in aqueous methanol and using the WATERGATE sequence for samples in 90% water. 2-D ^{1}H-^{15}N HSQC, 3-D ^{1}H-^{15}N-HSQC-NOESY, and 3-D ^{1}H-^{15}N-HSQC-TOCSY data were collected on a 1 mM sample of ^{15}N-labeled yU$^{\beta}$ at 298K, and the data were processed and assigned using Bruker XWINNMR and ANSIG software (*31*). Structures of yU$^{\beta}$ were generated using standard protocols within XPLOR (v3.1) (*32*). A total of 475 restraints was derived from *J*-coupling data and 2-D NOE data, and an ensemble of 100 structures was generated by the distance geometry protocol and was further refined using simulated annealing. Twenty structures were accepted, with no NOE violations greater than 0.2 Å, of which the hairpin portion of the 10 lowest energy structures is illustrated in Figure 2. A detailed description of the structure refinement calculations will be described subsequently. Structures were represented using MOLMOL (*33*).

Equilibrium Stability Measurements. Protein stability was determined by fluorescence measurements on 1−2 μM solutions of protein in 25 mM acetate buffer at pH 5.0. The change in fluorescence at 358 nm was monitored as a

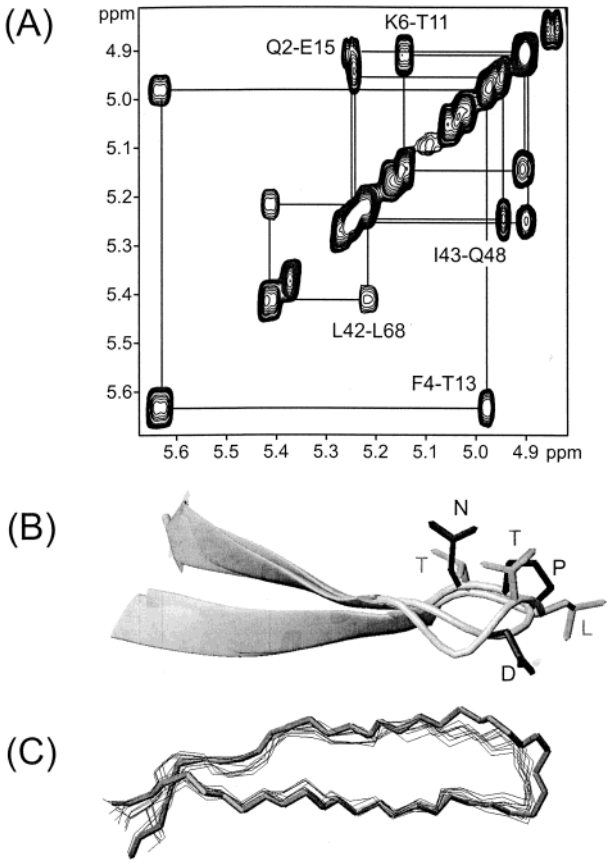

FIGURE 2: (A) Portion of the NOESY spectrum (300 ms mixing time) of yU$^{\beta}$ in D_2O solution (pH 5.0, 298 K) illustrating Hα−Hα cross-strand NOEs in antiparallel β-sheet. (B) Ribbon overlay of the β-hairpin portion (residues 1−16) of the averaged energy minimized structure of yU$^{\beta}$ with the native hairpin sequence taken from the X-ray structure of human ubiquitin (*16*); the position and orientation of the mutated side chains are shown [TLT (gray) → NPG (black)]. (C) Overlayed backbone of the hairpin portion of the 10 lowest energy NMR structures of yU$^{\beta}$ (thin lines) with the native hairpin backbone (thick line).

function of guanidinium hydrochloride concentration. The linear extrapolation method was employed (*34*−*38*) assuming that the stability varies with the concentration of denaturant [D], according to the expression $\Delta G^{D} = \Delta G_{eq} - m[D]$, where ΔG^{D} is the stability at a given [D], m is the constant of proportionality, and ΔG_{eq} is the stability in water alone. The slope of the denaturation plot at the midpoint of the transition (m-value) has been shown to correlate with the amount of hydrophobic surface area buried on folding (*38*). The fraction of folded protein F_f is derived from fluorescence measurements according to $F_f = (f_D - f_U)/(f_N - f_U)$, where f_D is the measured fluorescence at a given [D], and f_U and f_N are the limiting values for the unfolded and native states, respectively. The fraction folded was plotted against [D], and the midpoint of the unfolding transition $[D]_{50\%}$ for each mutant was determined by nonlinear least-squares fitting to the following expression:

$$F_f = \exp[m([D] - [D]_{50\%})/RT]/(1 + \exp[m([D] - [D]_{50\%})/RT]) \quad (1)$$

The equilibrium stability ΔG_{eq} was determined from the expression $\Delta G_{eq} = -m[D]_{50\%}$, where m for a set of mutants is assumed to be constant (10.28 ± 0.21 kJ mol^{-1} M^{-1}; mean value plus standard error from 18 data sets studied) (*37*). Small additional corrections were used to allow for a small denaturant dependence of the fluorescence of the unfolded state (*35*).

Kinetics Experiments. Kinetic unfolding and refolding measurements were performed using an Applied Photophysics Pi-star 180 spectrophotometer. Temperature was regulated to 298 K using a Neslab RTE-300 circulating programmable water bath. Excitation was at 281 nm using a 1 nm slit width. A band-pass filter was used to measure emitted light above 320 nm from a 2 mm path length cell. All kinetics experiments were performed in 25 mM acetate buffer, pH 5.0. Refolding experiments were performed by 1:10 dilution of unfolded protein (5−15 μM in 6.5 M GdnHCl) into buffered solutions of different GdnHCl concentrations yielding final concentrations ranging from 0.6 to 3.5 M at protein concentrations of 0.45−1.45 μM. For unfolding experiments, a buffered solution of native protein was unfolded by a 1:10 dilution to yield final concentrations of GdnHCl near or above the midpoint of the equilibrium unfolding transition (concentrations of GdnHCl in the range of 3.7−7.3 M). Kinetics measurements for both unfolding and refolding reactions were averaged four times at each GdnHCl concentration. In all cases, the GdnHCl concentration was determined using a refractometer (*34*).

Analysis of Kinetic Data. The kinetic traces were analyzed using a multiexponential fitting procedure (two or three components) in which one single component accounted for >90% of the change in fluorescence intensity. Minor slow-folding phases have previously been shown to arise from cis−trans proline isomerization. All data showed a good fit with randomly distributed residuals <0.05. Only the major component of the folding data was considered further. The kinetic data were analyzed assuming a two-state model using standard equations described in detail by others (*9*, *35*−*37*). The observed rate constant k_{obs} is the sum of the folding and unfolding rates, $k_{obs} = k_{U-N} + k_{N-U}$, where k_{obs} is dependent on [D] according to the following expression:

$$\ln k_{obs} = \ln[k_{N-U} \exp(m_{N-U}[D]/RT) + k_{U-N} \exp(m_{U-N}[D]/RT)] \quad (2)$$

The dependence of ln k_{obs} versus [D] gives extrapolated values for k_{N-U} and k_{U-N} in water alone, together with the slopes of the folding and unfolding components m_{N-U} and m_{U-N}.

RESULTS

Design of Mutant Ubiquitins. We have used the F45W mutant (yU*) as our wild-type protein for all biophysical studies because the unfolding of this mutant is associated with a large change in fluorescence intensity providing a sensitive probe for stability and kinetic studies (*19*−*21*). Subsequent mutations are set against this background mutation. The design of the ubiquitin mutants was based upon our earlier observations with the N-terminal 17 residue β-hairpin peptide that showed that mutation of the β-turn sequence was able to stabilize a nonnative conformation (*29*, *30*). The mutations are summarized as follows:

yU*:MQIFVK**TLTGK**TITLEV

yU$^{\beta}$: MQIFVK**NPDG**-TITLEV

yU$^{G-\beta}$:MQIFVK**NPDGK**TITLEV

Since the yU$^{\beta}$ mutations could result in destabilization of the protein either from removal of favorable tertiary contacts or through the introduction of new unfavorable interactions, we replaced TLTGK with NPDGK (yU$^{G-\beta}$). The latter enables us to assess possible effects of the TLT to NPD mutations on tertiary contacts within the context of the native type I G-bulged turn geometry.

NMR Analysis of the Folding of the Wild-Type and Mutant Ubiquitins. Native yU* gives a well-dispersed NMR spectrum with a large number of ring current-shifted methyl resonances between 0 and 0.7 ppm reflecting tertiary packing between aliphatic and aromatic side chains. Examination of the corresponding portion of the spectra of the mutants shows a practically identical shift dispersion, strongly indicating that core tertiary interactions are not disrupted by the changes in the hairpin sequence. A virtually complete backbone (NH and Hα) assignment for all three mutants has enabled us to identify numerous cross-strand Hα−Hα, NH−Hα, and NH−NH NOEs that unambiguously confirm the β-strand register. The interstrand Hα−Hα NOEs for yU$^{\beta}$ are shown in Figure 2A and demonstrate that the Q2-E15, F4-T13, and K6-T11 nativelike pairings are conserved in the folded state of yU$^{\beta}$ despite the strong propensity of the isolated hairpin peptide to fold to a nonnative strand alignment (Figure 1). The observation of chemical shift perturbations to the NH and Hα resonances of L68, V69, and residues within the N-terminal hairpin close to the modified turn (K6, T11, and I12) are consistent with some minor local structural adjustment. However, the identification of interstrand backbone NOEs between strands 1 and 5 in the region of the modified turn (N7 ↔ L68 and K6 ↔ H67/L68) confirms that there are no gross perturbations to the strand register or tertiary interactions. We have calculated a family of NMR structures for yU$^{\beta}$ using simulated annealing protocols within XPLOR (*32*) and will describe these studies in detail subsequently. The hairpin portion of the averaged energy minimized structure of yU$^{\beta}$, and 10 hairpin structures from the lowest energy NMR structures, are overlayed with the native sequence in Figure 2B,C. The NPDG sequence adopts a flattened, tight type I turn that slightly distorts the twisted conformation close to the β-turn region. In contrast, the native G-bulged type I turn, with its extra flexibility, readily adopts the required twist compatible with the β-strand alignment. Thus, despite the fact that the isolated β-hairpin peptide from yU$^{\beta}$ has a clear preference for a nonnative hairpin conformation, the β-strand alignment within the context of the intact protein appears to be strongly dictated by tertiary contacts in the hydrophobic core of the native structure and not by local secondary structure propensities. Parallel NMR studies of yU$^{G-\beta}$ unambiguously establish that the NPDGK turn sequence is adopting the type I G-bulged turn found in the native protein. This is particularly evident from strong sequential NH−NH NOEs between residues DGK, which are completely analogous to those between residues TGK in the native G-bulged turn (data not shown). Thus, the TLT → NPD mutations are readily accommodated without distortion.

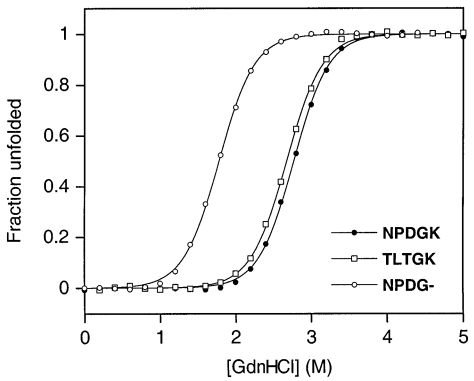

FIGURE 3: Equilibrium GdnHCl denaturation curves for ubiquitin mutants monitored by tryptophan fluorescence; the fraction unfolded is plotted vs [GdnHCl] at pH 5.0, 25 mM acetate buffer, 298 K for all three mutants yU* (TLTGK, open squares), yU$^{G-\beta}$ (NPDGK, black circles), and yU$^{\beta}$ (NPDG-, open circles); see data in Table 1.

Table 1: Equilibrium Stability Date for Ubiquitin Mutants (pH 5.0, 25 mM Acetate Buffer, 298 K) Determined by Guanidinium Chloride Denaturation Monitored by Changes in W45 Fluorescene

mutant	m_{eq}	$[D]_{50\%}$[a]	ΔG_{eq}[b]
TLTGK	10.3 ± 0.2	2.67	27.4 ± 0.6
NPDGK	10.5 ± 0.2	2.77	28.5 ± 0.6
NPDG-	10.4 ± 0.2	1.78	18.3 ± 0.4

[a] Denaturant concentration at the midpoint of the folding/unfolding transition, errors less than 0.01. [b] Equilibrium stability determined from the $[D]_{50\%}$ value using a mean *m*-value (and standard error) of 10.28 ± 0.21 kJ mol^{-1} M^{-1}.

Equilibrium Unfolding Studies. The equilibrium stability of yU* and the various mutants was determined by guanidinium chloride (GdnHCl)-induced denaturation in 25 mM acetate buffer at 298 K and pH 5.0 monitored by the change in tryptophan fluorescence at protein concentrations in the range of 1−2 μM (*24*, *25*). The data, showing the fraction folded, fit well to a two-state model enabling the transition midpoint ($[D]_{50\%}$) to be determined (*34*−*37*). The equilibrium stability ΔG_{eq} was calculated based on $[D]_{50\%}$ values, assuming that the slope of the denaturation plot at the midpoint of the transition (*m*-value) is common to all of the mutants studied, reflecting the same hydrophobic surface area buried on folding. Independent fitting to determine individual *m*-values shows this to be the case. Thus, $[D]_{50\%}$ values in this case provide a reliable method of comparing relative stabilities of mutants. For yU*, the unfolding transition occurs at 2.67 M GdnHCl, and the protein is fully unfolded above 4 M GdnHCl (Figure 3). The TLTGK → NPDGK (yU$^{G-\beta}$) mutant has a stability very similar to the native sequence ($\Delta\Delta G_{eq}$ = 1.1 kJ mol^{-1}). In contrast, the TLTGK → NPDG mutations in the β-turn, with a one residue deletion, result in a significant reduction in stability for yU$^{\beta}$ as judged by a shift in $[D]_{50\%}$ to 1.78 M, equivalent to a destabilization of yU$^{\beta}$ by 9 kJ mol^{-1} (see Table 1).

Folding and Unfolding Kinetics. Stopped-flow fluorescence was used to follow the refolding and unfolding of yU* and yU$^{\beta}$ under the same conditions used in equilibrium studies following 10-fold dilution to various final concentrations of denaturant (*35*−*37*). The data for yU* were fitted using a multiexponential analysis to account for minor slower folding phases that account for 10−15% of the change in fluorescence intensity. The latter has frequently been at-

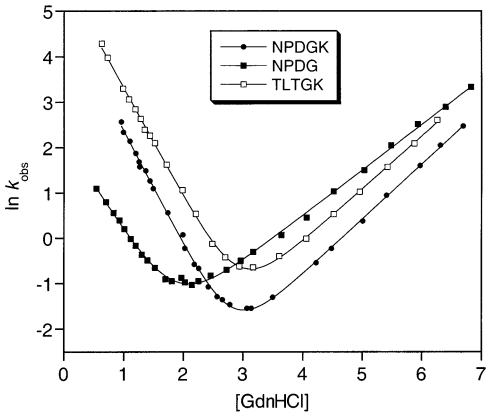

FIGURE 4: Chevron plots of refolding and unfolding kinetics for yU* (TLTGK), yU$^{G-\beta}$ (NPDGK), and yU$^{\beta}$ (NPDG) measured in 25 mM acetate buffer, pH 5.0 at 298 K showing the best fit to a two-state model.

tributed to the refolding of molecules with proline in a nonnative cis conformation (*21*, *39*−*41*), in agreement with the results of the double-jump studies of Krantz and Sosnick with human ubiqitin (*21*). For yU*, we considered only the fast folding phase and constructed a chevron plot of the natural logarithm of the observed rate constant (k_{obs}) versus [GdnHCl] (Figure 4). Both folding and unfolding components of the plot display a linear dependence on denaturant concentration. Extrapolation of the folding and unfolding data enables the rate constants to be determined in the absence of denaturant giving a refolding rate at 298 K and pH 5.0 of 304 s^{-1} and an unfolding rate of 0.0090 s^{-1} (see Table 2). The denaturant dependence of the folding (U-N) and unfolding rates (N-U) (m_{U-N} and m_{N-U}) determined from the slopes of the chevron plot have been shown to correlate with the difference in the exposed surface area between the transition state and the U and N states, providing a measure of the compactness of the transition state (β_{TS}), where $\beta_{TS} = m_{U-N}/(m_{N-U} + m_{U-N})$ (*38*, *42*, *43*). We estimate a value for β_{TS} for yU* of 0.67. A value of 0 is interpreted in terms of a transition state with a similar solvent accessibility to the unfolded state, whereas $\beta_{TS} = 1$ reflects a transition state as compact as the native state. The intermediate value of 0.67 is consistent with the value of 0.63 estimated for hU* by Krantz and Sosnick (*21*), indicating that the two transition states have similar degrees of compactness but with both somewhat less compact than the native state. How closely the kinetic data conform to a two-state model for folding can also be gauged from the agreement between stabilities determined by equilibrium measurements (ΔG_{eq}) and from the kinetic analysis (ΔG_{kin}) considering the ratio of the folding (k_{U-N}) and unfolding rates (k_{N-U}), where $\Delta G_{kin} = -RT \ln(k_{U-N}/k_{N-U})$ (*35*). From the kinetic data, we estimate $\Delta G_{kin} = -25.5$ (±0.8) kJ mol^{-1} for yU*, in good agreement with that determined from equilibrium GdnHCl-induced unfolding measurements, $\Delta G_{eq} = -27.4$ (±0.6) kJ mol^{-1}. Further, the kinetic *m*-value (m_{kin}) determined from the sum of the slopes of the data in Figure 4 ($m_{kin} = m_{U-N} + m_{N-U}$) should be equivalent to the equilibrium denaturation value. Again, there is good agreement (see Tables 1 and 2), consistent with the two-state folding model reported for human ubiquitin recently by Krantz and Sosnick (*21*) and determined by Jackson et al. (personal communication) under similar folding conditions.

Analysis of the kinetics of yU$^{\beta}$ was carried out under identical conditions to examine whether the large change in overall stability observed in equilibrium denaturation experiments originates from changes in the folding or unfolding rate, with implications for the role for the hairpin sequences in interactions in the transition state. It is apparent that the refolding arm of the chevron plot is significantly shifted giving an extrapolated refolding rate k_{U-N} of 9 s^{-1}, indicating that folding occurs 30 times more slowly than for the wild-type protein (Figure 4). In contrast, the unfolding data for the two proteins differ only by a factor of 3, demonstrating that the major portion of the reduction in stability is manifested in an increase in the barrier to folding. The data suggest an active role for hairpin formation in the folding nucleus of ubiquitin with the turn mutations frustrating the folding process by increasing the energy of the transition state. Calculation of kinetic and equilibrium *m*-values and β_{TS} values for yU$^{\beta}$ shows these to be very similar to those for yU*. We see no evidence for deviations from linearity of the plots of the folding and unfolding rate constants with concentration of denaturant, strongly suggesting that the transition state for folding is very similar to that of the wild-type protein and that folding still approximates well to a two-state model at protein concentrations <2 μM.

The yU$^{G-\beta}$ mutant, whose stability is very similar to that of the native sequence (yU*), shows small differences in refolding and unfolding kinetics (Figure 4). The extrapolated refolding rate constant lies within a factor of 3 of that observed for yU*, while the unfolding rate is within a factor of 2, indicating that these mutations result in only minor perturbations to stability and to kinetic barriers to folding. Calculation of β_{TS} from the slopes of the refolding and unfolding data shows the values to be identical, indicating that the mutations are not affecting the compactness of the transition state.

Effects of Methanol on Folding and Unfolding Kinetics. Several studies of the effects of organic cosolvents on folding rates have shown that partial stabilization of native secondary structure at low TFE or MeOH concentrations has the effect of initially accelerating folding rates but subsequently has a retarding effect due to the reduction in the magnitude of the hydrophobic effect, or as nonnative helical structure is induced in sequences destined to become β-strands, turns, or unstructured loops (*44*−*49*). The solvent perturbation approach has been used in a number of cases to examine whether secondary structure formation plays a key role in the transition state ensemble (*47*, *48*). We have already demonstrated from NMR studies of the N-terminal mutated peptide (residues 1−16) that the nonnative β-hairpin conformation is further stabilized in methanol (*29*). The results of others have demonstrated that cosolvents enhance native-like β-hairpin propensity in peptides with the native TLTGK β-turn sequence (*27*). The contrasting effects of cosolvents in stabilizing the native versus nonnative conformation for the two hairpin sequences may provide some additional insights into the role of secondary structure formation in the transition state ensemble. We have used both trifluoroethanol (TFE) and methanol for folding studies of yU* and yU$^{\beta}$. Methanol has some advantages over TFE in that it enhances native secondary structure propensities but is less prone to the nonspecific helix-inducing effects usually seen with TFE.

Table 2: Kinetics Data for the Refolding/Unfolding of Ubiquitin Mutants (pH 5.0, 298 K, 25 mM Acetate Buffer) Monitored by Changes in W45 Fluorescence Using Guanidinium Chloride Denaturation

mutant	k_{NU} (s^{-1})	m_{NU}	k_{UN} (s^{-1})	m_{UN}	ΔG_{kin} (kJ mol^{-1})[a]	β_{TS}[b]
TLTGK	0.0090 (±0.0008)	2876 (±44)	304 (±11)	5934 (±58)	−25.5 (±0.2)	0.67
NPDGK	0.0036 (±0.0003)	3004 (±43)	133 (±7)	6225 (±77)	−25.7 (±0.2)	0.67
NPDG-	0.030 (±0.002)	2482 (±27)	9 (±1)	5135 (±134)	−14.2 (±0.2)	0.67

[a] ΔG_{kin} determined from $-RT \ln(k_{UN}/k_{NU})$. [b] β_{TS} values determined from $m_{UN}/(m_{UN} + m_{NU})$.

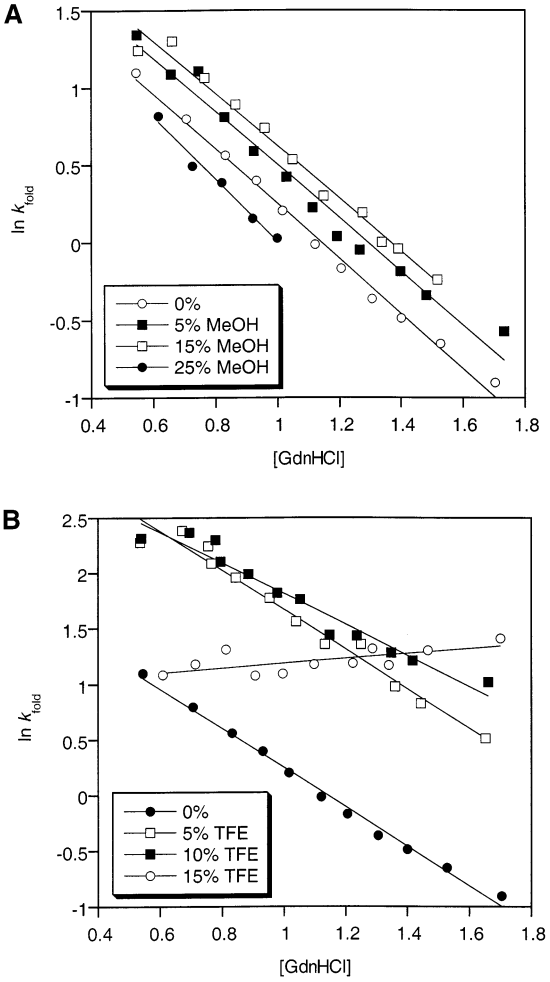

FIGURE 5: (A) Effects of methanol (% v/v) on refolding kinetics of yU^{β} in 25 mM acetate, pH 5.0 at 298 K. (B) Effects of TFE (% v/v) on refolding kinetics under identical conditions to panel A.

There is no significant effect on the folding rate for yU* up to 15% (v/v) methanol; however, 25% (v/v) of cosolvent produces a 2-fold retardation of the folding rate. The effects on the unfolding kinetics are slightly more pronounced resulting in accelerated unfolding by up to a factor of 3 over this solvent range. The slopes of the chevron plots (folding and unfolding) show only small perturbations. Surprisingly, the results for yU^{β} (containing the NPDG turn mutation) are quite similar with a modest <2-fold acceleration of the folding rate up to 15% (v/v) methanol and a deceleration at 25% (v/v) (Figure 5A). In TFE, the effects are more pronounced, reflecting its stronger structure-inducing characteristics. The effects on the folding kinetics of yU* are clearly complicated; 5% (v/v) produces a significant acceleration of the folding rate; however, the data now show distinct curvature indicating deviation from a simple two-state model. At higher concentrations of TFE, we see marked changes in the slope of the refolding data with the folding rate becoming independent of the GdnHCl concentration. Parallel CD studies show that between 20 and 30% TFE, yU* is partially denaturated with an increase in nonnative helical structure characteristic of the N- to A-state transition previously described for ubiquitin (*50*−*52*). The effect of 5−10% TFE on the folding kinetics of yU^{β} is to produce a significant acceleration of folding by a factor of ∼4 with little evidence of deviation from the two-state model (Figure 5B). The denaturing effects of TFE take effect at 15% (v/v), where again we see a folding rate that becomes independent of GdnHCl concentration with CD data identifying solvent-induced helical structure. The data suggest deviations from the two-state folding model as partially folded states become significantly stabilized. Although the effects of cosolvent on the folding kinetics are complex at high cosolvent concentrations, the data clearly show that the folding kinetics for yU^{β} is modestly accelerated at low concentrations of MeOH and TFE.

NMR Analysis of Residual Structure in the N-Terminal Hairpin of yU^{β} in Denaturants and Methanol. The N-terminal peptide, corresponding to residues 1−35 of yU^{β} and containing the TLTGK → NPDG turn mutations, has been investigated by NMR for evidence of residual structure under folding conditions in water and in 5−25% (v/v) methanol. As previously described for the isolated hairpin (*17*, *18*), Hα chemical shift deviations from random coil values (up to 0.7 ppm for Ile12) show clear evidence for β-hairpin formation, supported by Hα−Hα cross-strand contacts between Q2-V16, F4-L14, and K6-I12 and numerous side chain interactions. In contrast, residues in the adjoining loop (residues 17−20) and α-helical domain (residues 21−35) show very small perturbations to Hα shifts indicating at best the possibility of transient helical structure. AGADIR predictions (*53*) of helical content across the 21−35 portion of the sequence also suggest little intrinsic propensity (<1%) to adopt the native helical structure.

Earlier studies of ubiquitin peptide fragments derived from the native sequence have shown the hairpin portion (residues 1−17) to fold weakly in aqueous solution with the native secondary structure propensity dramatically enhanced by the addition of methanol (*27*, *28*). The effect of cosolvents on the folding of the 1−35 peptide with the NPDG turn at concentrations of methanol between 15 and 25% v/v is to significantly stabilize nonnative hairpin conformation, as evident from increased Hα shift deviations and an abundance of cross-strand NOEs compatible with this conformation. However, close examination of the NOESY data reveals a number of much weaker Hα−Hα NOEs (F4 ↔ T13 and K6 ↔ T11) and side chain interactions, in particular F4 to T11/T13, that are compatible with a minor conformer with a nativelike β-strand alignment (Figure 6). This minor hairpin conformer is not detected in the NOESY data recorded in aqueous solutions suggesting that the cosolvent enhances the

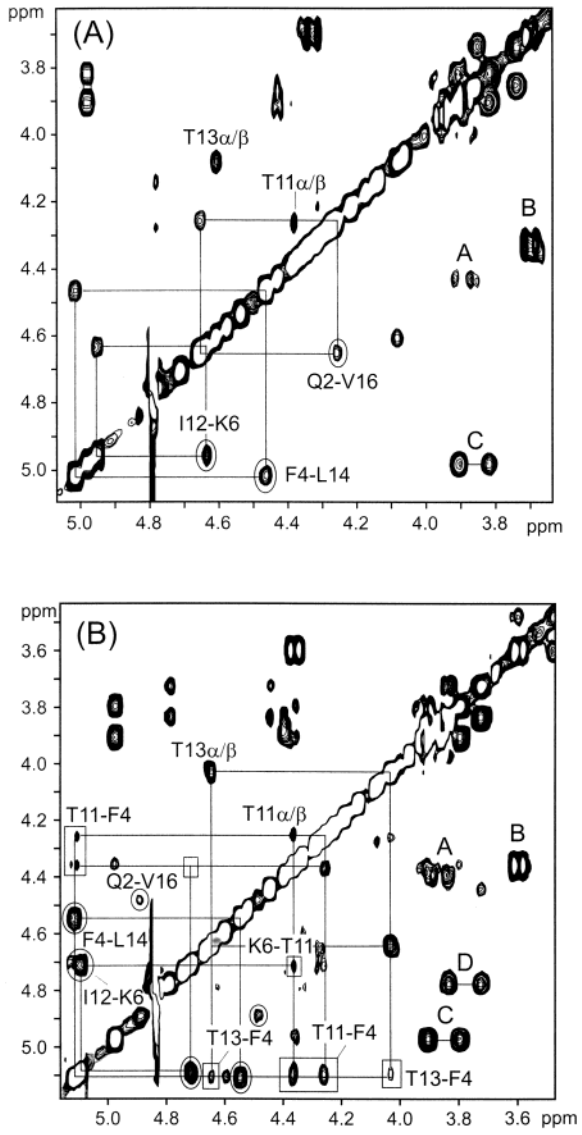

FIGURE 6: Plots of the Hα−Hα region of the 2-D NOESY spectra of peptide U(1−35) containing the TLTGK → NPDG turn mutations: (A) NOESY data (200 ms) recorded in aqueous solution, pH 5.0 at 298K, and (B) in 25% (v/v) methanol under the same conditions. Cross-strand NOEs corresponding to the nonnative hairpin alignment are clearly identified with circles in both panels A and B. In panel B, additional cross-peaks are highlighted (in boxes) that correspond to a minor population of a nativelike β-hairpin conformer with the strand alignment shown in Figure 1A. Other peaks identified in panels A and B are labeled as follows: A, S19α/β; B, G10 α/α; C, N7α-P8δ; and D, E17α-P18δ.

population of both the native and the nonnative hairpin conformation by promoting hydrogen bonding interactions. In addition, the cosolvent simultaneously enhances nativelike helical structure in the 21−35 portion of the peptide sequence as evident from both Hα chemical shift data and CD studies of 1−35 (*27*). The observation of NH_i-NH_{i+1} NOEs and medium range $H\alpha_i-NH_{i+3}/NH_{i+4}$ NOEs within the 21−31 region of the sequence are indicative of well-formed helical structure largely in the N-terminal part of the native sequence.

DISCUSSION

Local versus Nonlocal Interactions in Protein Stability, Specificity, and Folding Kinetics. Mutation of the β-turn sequence of the N-terminal β-hairpin of ubiquitin from TLTGK to an NPDG type I turn enhances the secondary structure propensity of the isolated hairpin but by inducing nonnative alignment of the two β-strands (see Figure 1). The driving force for this conformational transition appears to originate from two key factors. First, the type I turn is not compatible with the right-handed twist of the β-hairpin. Gellman has illustrated this nicely within model hairpin systems by showing that switching the turn conformation from type I ^{L}Pro-Xaa to type I′ ^{D}Pro-Xaa promotes folding by changing the conformational preference of the backbone to one compatible with the twisted β-strand alignment (*54*, *55*). In contrast, the G-bulged type I turn is more flexible and has a high statistical occurrence in β-hairpins (*30*, *56*). Second, the strand realignment that results in nonnative cross-strand pairing of side chains appears to have a net stabilizing effect on hairpin conformation. In particular, the Phe−Leu pair results in significant hydrophobic surface burial and stabilizing van der Waals contacts between residues that are on opposite faces of the hairpin in the native conformation. These close contacts are evident from the substantial upfield ring current shifts observed on the Leu $C_\delta H_3$ resonances (∼0.3 ppm). These two factors result in a β-hairpin peptide that is 70−80% folded in water and highly resistant to denaturation by urea (*29*, *30*). Thus, one important role for the native TLTGK turn sequence may be to prevent the formation of these nonnative hydrophobic contacts by having a bulged turn that is resistant to further expansion.

In contrast, our NMR analysis shows that the mutated hairpin, when placed in the context of the rest of the ubiquitin sequence, adopts a well-defined structure in which the native strand alignment has been enforced. This clearly shows that the specificity of the folded structure is independent of the local interactions that define the nonnative β-sheet propensity of the isolated hairpin peptide (*5*, *6*). However, denaturation experiments show that the protein is destabilized by ∼9 kJ mol^{-1}, indicating that local interactions play an important role in modulating stability. A large proportion of this difference in stability is manifested in a 30-fold deceleration of the folding reaction, with a more modest 3-fold acceleration of the unfolding reaction. These data suggest that a nativelike hairpin conformation is important in the rate-limiting step for folding.

Destabilization of yU$^{\beta}$: Effects of Other β-Turn Mutations on Stability and Kinetics. The effect of the turn mutation on protein stability can, in principle, be partitioned among a number of factors relating to both local interactions, including changes to secondary structure propensities and conformational strain in the turn, and effects on longer range tertiary contacts. The latter could result in destabilization either from removal of favorable contacts from residue side chains within the turn region or from the introduction of new unfavorable tertiary contacts. We have investigated the latter possibilities by replacing the largely solvent-exposed native TLTGK turn with NPDGK (yU$^{G-\beta}$). NMR studies of the yU$^{G-\beta}$ mutant show that the NPDGK turn adopts the same G-bulged type I turn as the native TLTGK sequence enabling us to assess the impact of the TLT to NPD mutations on nonlocal interactions within the folded protein. The NMR data show that the NPD residues are readily incorporated within the G-bulged type I turn with minimal distortion of the structure. Moreover, stability studies show that the yU$^{G-\beta}$ mutant is stabilized as compared to yU* by 1.1 kJ mol^{-1}. This small

difference could arise from the entropic effects of inserting a proline residue in the turn sequence. Further, the kinetic data are very similar for yU* and $yU^{G-\beta}$: we see a small deceleration of the refolding rate and slightly slower unfolding kinetics (Table 2). Thus, introduction of the NPD mutations do not appear to have a significant effect on stability or kinetics. In all of the mutants studied, estimates of the degree of compactness of the transition state (β_{TS}) from the slopes of the chevron plot give very similar values (Table 2), indicating that the transition state is not significantly perturbed by the turn mutations. The kinetic data for $yU^{G-\beta}$ are consistent with two-state kinetics at protein concentrations <2 μM. Thus, within the context of the mutations studied here, we conclude that nonlocal contacts involving mutated residues in the turn appear to have a relatively small effect on the stability and kinetics of yeast ubiquitin.

Stabilization of Native and Nonnative Secondary Structure by Cosolvents. Several studies on the effects of organic cosolvents on folding rates have shown that partial stabilization of native secondary structure at low TFE or MeOH concentrations has the effect of accelerating folding rates in cases where elements of secondary structure are forming in the transition state ensemble (*46*, *48*). Retarded folding rates at higher cosolvent concentrations have been attributed to either nonspecific effects in stabilizing nonnative helical structure in portions of the sequence or through reduction of the magnitude of the hydrophobic effect (*48*). Studies of 13 proteins that fold in a two-state manner show that the extent of acceleration correlates closely with the number of local backbone hydrogen bonds in the native structure (*46*), while the extent of deceleration can be related to the amount of accessible surface area buried on folding. On the basis of this model, we would predict that MeOH and TFE would also initially accelerate the folding of yU* by stabilizing native β-hairpin and α-helical structure, as is evident from studies of the isolated peptides. However, if the stabilization of nativelike secondary structure plays a key role in accelerating refolding kinetics, then the effect of MeOH/TFE on the kinetics of yU^{β} may be complicated by the stabilization of both native and nonnative conformations in different portions of the peptide sequence. Alternatively, studies of FKBP12 and a number of mutants with substitutions of nonpolar residues have shown that the pathway for folding is unaffected by cosolvents and that rather than stabilizing elements of secondary structure in the transition state, the effects on folding and unfolding rates appear to be a result of global effects that desolvate and destabilize the unfolded state (*47*, *57*).

The folding kinetics for yU* and yU^{β} has been determined in the presence of cosolvents [0−25% aqueous MeOH (v/v) and 0−15% TFE (v/v)] under otherwise identical conditions. The accelerating effects of MeOH on the refolding of yU^{β} and yU* are very small (<2-fold) up to 15% cosolvent, with a subsequent reduction in folding rate at higher concentrations. However, both proteins show a significant increase in unfolding rate over the entire range of concentrations consistent with a decrease in the stability of the native state as the effects of cosolvent reduce the magnitude of the hydrophobic effect. The more pronounced effects of TFE in enhancing secondary structure propensity results in a larger effect on the folding kinetics; the folding rate for yU^{β} is enhanced in 5−10% TFE solution by a factor of ~4. Above this concentration, the refolding kinetics becomes independent of denaturant concentration as the protein adopts a cosolvent-induced partially denaturated state with an increase in nonnative helical structure characteristic of the N- to A-state transition previously described for ubiquitin (*50*−*52*). The effects of cosolvent on the kinetics of yU^{β} clearly show that refolding is accelerated at low concentrations of MeOH or TFE.

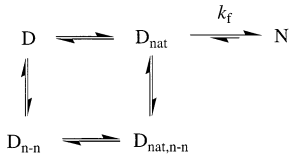

FIGURE 7: Schematic representation of the equilibria present under refolding conditions in the denatured state (D) between various species that are rapidly interconverting and containing residual native contacts (nat), nonnative contacts (n-n), or both (nat, n-n). N is the native folded state, and k_f is the folding rate constant.

The previous observations are perhaps surprising given the NMR results with the C-terminal peptide fragment of yU^{β} that show that nonnative β-hairpin conformation is further stabilized by cosolvents. How then do we rationalize the observation that the refolding kinetics of yU^{β} are accelerated in the presence of organic cosolvents? Chiti et al. (*48*) have recently discussed the contribution of nonnative conformations to the conformational ensemble of the denatured state (D); this model proves useful in the current context if the denatured state is considered as an ensemble of states containing various proportions of local secondary structure. This could be either nativelike structure (D_{nat}), nonnative (D_{n-n}), a mixture of the two ($D_{nat,n-n}$), or the polypeptide could be fully denatured (D) under refolding conditions with these various partially folded states in rapid equilibrium with each other. The barriers to interconversion in the denatured state are assumed to be negligible as compared with the transition to the native state (N), so the former are not rate-limiting. Thus, the denatured ensemble contains a set of independent equilibria with the relative populations of the various species dependent on the various equilibrium constants. A reasonable approximation is that the folding reaction (rate constant k_f) is likely to be faster from D_{nat}, where nativelike contacts are formed in the denatured state, than from any other state. Thus, the set of equilibria shown in Figure 7 are considered.

From the perspective of understanding the difference in the kinetics observed between yU* and yU^{β}, the ~30-fold deceleration in refolding rate for yU^{β} in water can be rationalized in terms of the stabilization of nonnative conformations of yU^{β} in the denatured state that deplete the pool of species present with nativelike contacts (D_{nat}). The population of all species in the denatured state that contain either native or nonnative structure, or both, is likely to increase in the presence of low concentrations of cosolvents. Whether or not the rate of folding of yU^{β} is accelerated depends on the effects of the cosolvent on the population of D_{nat}. Thus, we can rationalize the observed accelerated refolding rate for yU^{β} in terms of the increase in the population of D_{nat} even though the population of D_{n-n} and $D_{nat,n-n}$ may also be significantly enhanced over those present in water alone. Our NMR results on the C-terminal peptide

fragment U(1−35) show that the nonnative β-hairpin structure (residues 1−16) persists in aqueous solution (i.e., D_{n-n} is significantly populated). We see that MeOH and TFE enhance the native helical propensity of the 21−31 portion of the sequence, as well as further stabilizing the nonnative β-hairpin conformation such that $D_{nat,n-n}$ is significantly populated. However, the data also reveal that the population of species with the nativelike β-strand alignment in the hairpin sequence (D_{nat}) is increased. Thus, all partially structured species (D_{nat}, $D_{nat,n-n}$, and D_{n-n}) appear to be in greater abundance in the presence of cosolvent. However, the accelerated folding of yU^{β} at low cosolvent concentrations appears to correlate with the small increase in the population of species with nativelike local interactions (D_{nat}) despite the increase in the population of other nonnative species in the denatured ensemble that do not contribute to the folding reaction.

In conclusion, hierarchical models suggest that rapid formation of nativelike secondary structure in the denatured state should facilitate and accelerate folding by reducing the configurational entropy en route to the transition state (*1*−*3*, *48*). In support of this model, studies of short protein fragments and designed peptides show that elements of secondary structure can form autonomously under folding conditions on a very rapid time scale (*54*, *55*). Moreover, site-directed mutagenesis has shown that secondary structure propensities in proteins can be fined-tuned to accelerate folding rates in accord with the importance of local folding events in directing the folding reaction (*10*−*12*, *14*). The solvent perturbation approach provides a low resolution method of enhancing local hydrogen bonding propensities to examine the role of secondary structure formation in the rate-limiting step (*45*−*49*). We have used a combination of these approaches to examine the effects on stability and folding kinetics of introducing a nonnative structural propensity into the N-terminal β-hairpin sequence of yeast ubiquitin. Mutating the native TLTGK β-turn to NPDG induces a β-strand misalignment resulting in nonnative side chain pairings in the stabilized β-hairpin (*29*, *30*). Although these local interactions dictate conformational preferences in the isolated peptide, they are not sufficient to enforce nonnative conformation in the native protein, indicating that nonlocal tertiary interactions are the main determinants of β-sheet secondary structure (*5*, *12*, *15*). The enforcement of the native β-strand alignment has the effect of destabilizing the native state and effectively increases the folding barrier resulting in a ~30-fold deceleration of the folding reaction as compared with the wild-type protein. However, cosolvents have the effect of accelerating the folding reaction of these mutants despite an apparent increase in stability of nonnative interactions. NMR studies show that all partially folded species in solution, both with nonnative and with native local interactions, appear to be more highly populated, offering one possible explanation for the accelerated folding rate. The observation that mutations in the β-hairpin that perturb the population of nativelike species in the denatured ensemble can have a large effect on the folding kinetics suggests that nativelike interactions are present within the hairpin sequence in the transition state ensemble, emphasizing the importance of local interactions in directing the folding process.

REFERENCES

1. Baldwin, R. L., and Rose, G. (1999) Is protein folding hierarchic? Local structure and peptide folding, *Trends Biochem. Sci. 24*, 77−83.
2. Brockwell, D. J., Smith, D. A., and Radford, S. E. (2000) Protein folding mechanisms: new methods and emerging ideas, *Curr. Opin. Struct. Biol. 10*, 16−25.
3. Honig, B. (1999) Protein folding: from the Levinthal paradox to structure prediction, *J. Mol. Biol. 293*, 283−293.
4. Jackson, S. E. How do small single domain proteins fold? (1998) *Folding Des. 3*, R81−R91.
5. Minor, D. L., Jr., and Kim, P. S. (1996) Context-dependent secondary structure formation of a designed protein sequence, *Nature 380*, 730−734.
6. Cregut, D., Civera, C., Macias, M. J., Wallon, G., and Serrano, L. (1999) A tale of two secondary structure elements: when a β-hairpin becomes an α-helix, *J. Mol. Biol. 292*, 389−401.
7. Myers, J. K., and Oas, T. G. (2001) Preorganized secondary structure as an important determinant of fast protein folding, *Nat. Struct. Biol. 8*, 552−558.
8. Kim, D. E., Yi, Q., Gladwin, S. T., Goldberg, J. M., and Baker, D. (1998) The single helix in protein L is largely disrupted at the rate-limiting step in folding, *J. Mol. Biol. 284*, 807−815.
9. Viguera, A.-R., and Serrano, L. (2001) Bergerac-SH3: frustration induced by stabilizing the folding nucleus, *J. Mol. Biol. 311*, 357−371.
10. Viguera, A.-R., Villegas, V., Aviles, F. X., and Serrano, L. (1997) Favourable nativelike helical local interactions can accelerate protein folding, *Fold. Des. 2*, 23−33.
11. Lopez-Hernandez, E., Cronet, P., Serrano, L., and Munoz, V. (1997) Folding kinetics of Che Y mutants with enhanced native α-helix propensities, *J. Mol. Biol. 266*, 610−620.
12. Munoz, V., and Serrano, L. (1996) Local versus nonlocal interactions in protein folding and stability—an experimentalist's point of view, *Fold. Des. 1*, R71−R77.
13. Burton, R. E., Huang, G. S., Daugherty, M. A., Calderone, T. L., and Oas, T. G. (1996) Microsecond protein folding through a compact transition state, *J. Mol. Biol. 263*, 311−322.
14. Nauli, S., Kuhlman, B., and Baker, D. (2001) Computer-based redesign of a protein folding pathway, *Nat. Struct. Biol. 8*, 602−605.
15. Prieto, J., Wilmans, M., Jimenez, M. A., Rico, M., and Serrano, L. (1997) Nonnative local interactions in protein folding and stability: introducing a helical tendency in the all β-sheet α-spectrin SH3 domain, *J. Mol. Biol. 268*, 760−778.
16. Vijay-Kumar, S., Bugg, C. E., Wilkinson, K. D., Vierstra, R. D., Hatfield, P. M., and Cook, W. J. (1987) Comparison of the three-dimensional structures of human, yeast, and oat ubiquitin, *J. Biol. Chem. 262*, 6396−6399.
17. Briggs, M. S., and Roder, H. (1992) Early hydrogen bonding events in the folding of ubiquitin, *Proc. Natl. Acad. Sci. U.S.A. 89*, 2017−2021.
18. Gladwin, S. T., and Evans, P. A. (1996) Structure of the very early protein folding intermediates: new insights through a variant of hydrogen exchange labeling, *Fold. Des. 1*, 407−417.
19. Khorasanizadeh, S., Peters, I. D., and Roder, H. (1993) Stability and folding of a tryptophan containing a mutant of ubiquitin, *Biochemistry 32*, 7054−7063.
20. Khorasanizadeh, S., Peters, I. D., and Roder, H. (1996) Evidence for a three-state model of protein folding from kinetic analysis of ubiquitin variants with altered core residues, *Nat. Struct. Biol. 3*, 193−205.
21. Krantz, B. A., and Sosnick, T. R. (2000) Distinguishing between two-state and three-state models for ubiquitin folding, *Biochemistry 39*, 11696−11701.
22. Ermolenko, D. N., Thomas, S. T., Aurora, R., Gronenborn, A. M., and Makhatadze, G. I. (2002) Hydrophobic interactions at the C-cap position of the C-capping motif of α-helices, *J. Mol. Biol. 322*, 123−135.
23. Thomas, S. T., and Makhatadze, G. I. (2000) Contribution of the 30/36 hydrophobic contact at the C-terminus of the α-helix to the stability of the ubiquitin molecule, *Biochemistry 39*, 10275−10283.
24. Loladze, V. V., Ermolenko, D. N., and Makhatadze, G. I. (2002) Thermodynamic consequences of burial of polar and nonpolar amino acid residues in the protein interior, *J. Mol. Biol. 320*, 343−357.

25. Ibarra-Molero, B., Loladze, V. V., Makhatadze, G. I., and Sanchez-Ruiz, J. M. (1999) Thermal versus guanidine-induced unfolding of ubiquitin. An analysis in terms of the contributions from charge−charge interactions to protein stability, *Biochemistry 38*, 8138−8149.
26. Loladze, V. V., Ibarra-Molero, B., Sanchez-Ruiz, J. M., and Makhatadze, G. I. (1999) Engineering a thermostable protein via optimization of charge−charge interactions on the protein surface, *Biochemistry 38*, 16419−16423.
27. Cox, J. P. L., Evans, P. A., Packman, L. C., Williams, D. H., and Woolfson, D. N. (1993) Dissecting the structure of a partially folded protein. CD and NMR studies of peptides from ubiquitin, *J. Mol. Biol. 234*, 483−492.
28. Zerrela, R., Evans, P. A., Ioniodes, J. M. C., Packman, L. C., Trotter, B. W., Mackay, J. P., and Williams, D. H. (1999) Autonomous folding of a peptide corresponding to the N-terminal β-hairpin of ubiquitin, *Protein Sci. 8*, 1320−1331.
29. Searle, M. S., Williams, D. H., and Packman, L. C. (1995) A short linear peptide derived from the N-terminal sequence of ubiquitin folds into a water-stable nonnative β-hairpin, *Nat. Struct. Biol. 2*, 999−1006.
30. Jourdan, M., Griffiths-Jones, S. R., and Searle, M. S. (2001) Folding of a β-hairpin peptide derived from the N-terminus of ubiquitin: conformational preferences of β-turn residues dictate nonnative β-strand interactions, *Eur. J. Biochem. 267*, 3539−3548.
31. Kraulis, P. J. (1989) ANSIG: A program for the assignment of protein ^{1}H 2-D NMR spectra by interactive computer graphics, *J. Magn. Reson. 24*, 627−633.
32. Brunger, A. T. (1992) *X-PLOR version 3.1, A system for X-ray crystallography and NMR*, Yale University Press, New Haven, CT.
33. Koradi, R., Billeter, M., and Wuthrich, K. (1996) MOLMOL: a program for display and analysis of macromolecular structures, *J. Mol. Graph. 14*, 51−55.
34. Pace, N. C., and Scholtz, J. M. (1997) in *Protein Structure—A Practical Approach*, 2nd ed. (Creighton, T. E., Ed.) IRL Press, New York.
35. Ferguson, N., Capaldi, A. P., James, R., Kleanthous, C., and Radford, S. E. (1999) Rapid folding with and without populated intermediates in the homologous four-helix proteins Im7 and Im9, *J. Mol. Biol. 286*, 1597−1608.
36. Jackson, S. E., and Fersht, A. R. (1991) Folding of chymotrypsin inhibitor 2: Evidence for a two-state transition state, *Biochemistry 30*, 10428−10435.
37. Main, E. R. G., and Jackson, S. E. (1999) Folding of FKBP12: pathway of folding and characterisation of the transition state. *J. Mol. Biol. 291*, 429−444.
38. Myers, J. K., Pace, C. N., and Scholtz, J. M. (1995) Denaturant *m*-values and heat capacity changes: relation to changes in accessible surface areas of protein folding, *Protein Sci. 4*, 2138−2148.
39. Maki, K., Ikura, T., Hayano, T., Takahashi, N., and Kuwajima, K. (1999) Effects of proline residues on the folding of *Staphylococcal* nuclease, *Biochemistry 38*, 2213−2223.
40. Jackson, S. E., and Fersht, A. R. (1991) Folding of chymotrypsin inhibitor-2. 2.Influence of proline isomerization on the folding kinetics and thermodynamic characterization of the transition state of folding, *Biochemistry 30*, 10436−10443.
41. Eyles, S. J., and Gierasch, L. M. (2000) Multiple roles of proline residues in structure and folding, *J. Mol. Biol. 301*, 737−747.
42. Matouschek, A., Kellis, J. T., Serrano, L., and Fersht, A. R. (1989) Mapping the transition state and pathway of protein folding by protein engineering, *Nature 340*, 122−126.
43. Serrano, L., Matouschel, A., and Fersht, A. R. (1992) The folding of an enzyme. III. Structure of the transition state for unfolding of Barnase analyzed by a protein engineering procedure, *J. Mol. Biol. 224*, 805−818.
44. Buck, M. (1998) Trifluorethanol and colleagues: cosolvents come of age. Recent studies with peptides and proteins, *Q. Rev. Biophys. 31*, 297−355.
45. Lu, H., Buck, M., Radford, S. E., and Dobson, C. M. (1997) Acceleration of the folding of hen lysozyme by trifluoroethanol, *J. Mol. Biol. 265*, 112−117.
46. Hamada, D., Chiti, F., Guijarro, J. I., Kataoka, M., Taddei, N., and Dobson, C. M. (2000) Evidence concerning rate-limiting steps in protein folding from the effects of trifluoroethanol, *Nat. Struct. Biol. 7*, 58−61.
47. Main, E. R. G., and Jackson, S. E. (1999) Does trifluoroethanol affect folding pathways and can it be used as a probe of structure in transition states? *Nat. Struct. Biol. 6*, 831−835.
48. Chiti, F., Taddei, N., Webster, P., Hamada, D., Fiaschi, T., Ramponi, G., and Dobson, C. M. (1999) Acceleration of the folding of acylphosphatase by stabilization of local secondary structure, *Nat. Struct. Biol. 6*, 380−387.
49. Ionescu, R. M., and Matthews, C. R. (1999) Folding under the influence, *Nat. Struct. Biol. 6*, 304−307.
50. Harding, M., Williams, D. H., and Woolfson, D. N. (1991) Characterization of a partially denatured state of a protein by 2-D NMR reduction of the hydrophobic interaction in ubiquitin, *Biochemistry 30*, 3120−3128.
51. Woolfson, D. N., Cooper, A., Harding, M. M., Williams, D. H., and Evans, P. A. (1993) Protein folding in the absence of the solvent ordering contribution to the hydrophobic interaction, *J. Mol. Biol. 229*, 502−511.
52. Jourdan, M., and Searle, M. S. (2001) Insights into the stability of native and partially folded states of ubiquitin: effects of cosolvents and denaturants on the thermodynamics of protein folding, *Biochemistry 40*, 10317−10325.
53. Lacroix, E., Viguera, A. R., and Serrano, L. (1998) Elucidating the folding problem of α-helices: Local motifs, long-range electrostatics, ionic strength dependence, and prediction of NMR parameters, *J. Mol. Biol. 284*, 173−191.
54. Gellman, S. H. (1999) Minimal model systems for β-sheet secondary structure in proteins, *Curr. Opin. Chem. Biol. 2*, 717−725.
55. Searle, M. S. (2001) Peptide models of protein β-sheets: design, folding, and insights into stabilizing weak interactions, *J. Chem. Soc., Perkin Trans. 2 1*, 1−10.
56. Wilmot, C. M., and Thornton, J. M. (1988) Analysis and prediction of the different types of β-turns in proteins, *J. Mol. Biol. 203*, 221−232.
57. Kentsis, A., and Sosnick, T. R. (1998) Trifluoroethanol promotes helix formation by destabilizing backbone exposure: desolvation rather than native hydrogen bonding defines the kinetic pathway of dimeric coiled−coil folding, *Biochemistry 37*, 14613−14622.

BI030147D